3D Printed Substrate Integrated Waveguide Filters with Locally Controlled Dielectric Permittivity

Cristiano Tomassoni
Dept. of Engineering
University of Perugia
Perugia, Italy

Ryan Bahr, Manos Tentzeris
School of Electrical and Computer Engn.
Georgia Institute of Technology
Atlanta, USA

Maurizio Bozzi, Luca Perregrini
Dept. of Electrical, Computer and Biomedical Engineering
University of Pavia, Pavia, Italy

***Abstract*—This paper presents, for the first time, the implementation of SIW filters by 3D printing manufacturing technique. The possibility of locally modifying the effective dielectric permittivity by changing the infill factor of the printing process is exploited and demonstrated. This allows adopting a single filament material to obtain different permittivity values in the various portions of a microwave component. Moreover, the variation of the infill factor allows reducing the dielectric loss tangent of the material: this permits increasing the quality factor of cavity filters even by using the same material. These features are illustrated through the design and experimental verification of two SIW filters, with identical frequency response but fabricated with different infill factor of the printing process, via fused deposition modeling (FDM).**

***Keywords*—Substrate integrated waveguide, 3D printing, fused deposition modeling, effective dielectric permittivity.**

I. Introduction

Additive Manufacturing (AM), often associated with 3D printing, is an emerging class of manufacturing processes that join materials to make objects from 3D models, usually layer upon layer, as opposed to subtractive manufacturing technologies. AM is becoming popular for many applications (ranging from anatomical models to building construction), contributing to the third industrial revolution, with a completely new model of industry and production [1]-[3].

In the field of microwave components and systems, AM offers several advantages, including rapid prototyping, unprecedented design flexibility, and low cost for facilities and materials [4],[5]. Moreover, the possibility to embed wireless systems in everyday life objects opens new perspective for the Internet of Things [6]. Initially adopted for rapid prototyping, to test the design before the final product development, AM technologies have rapidly improved towards the complete (one-pass) manufacturing of end-use components.

Among the variety of 3D printing technologies, fused deposition modeling (FDM) is one of the most promising approach for printing polymers for microwave applications. FDM is an extrusion-based 3D-printing technique: a plastic filament is heated and extruded from a nozzle. The extruder precisely lays down the material to form 2D layers of material that hardens immediately after extrusion. The overlap of 2D layers results into the final 3D printed structure. The technology is simple and cost effective, and commercial printers deposit layers with height of 100 μm, a typical planar resolution of 50 μm and a vertical accuracy down to 20 μm. In addition, a unique feature of FDM is the capability of changing the density of the printed material, by varying the infill percentage, from 100% to roughly 10% [7].

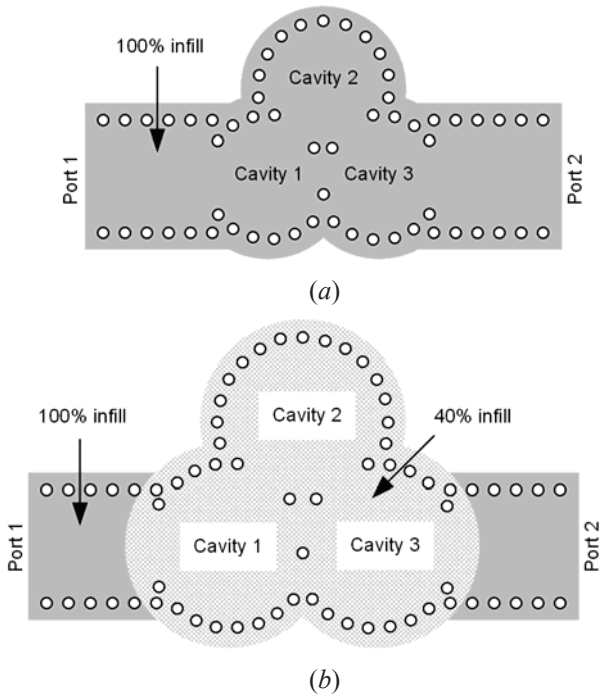

Fig. 1. Geometry of the 3D printed three-pole filters: (*a*) filter entirely fabricated with 100% infill; (*b*) filter fabricated partly with 100% infill and partly 40% infill.

This last feature of FDM technology is exploited in this paper, with a twofold aim. The variation of the infill factor permits to obtain different permittivity values in the various portions of a microwave component, which can be used for the

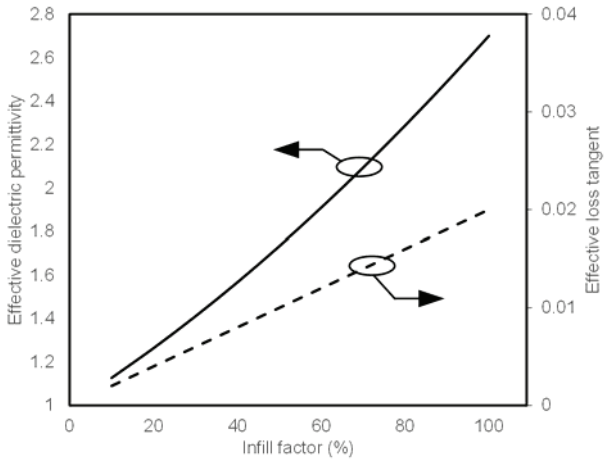

Fig. 2. Variation of effective dielectric permittivity and loss tangent versus the infill factor.

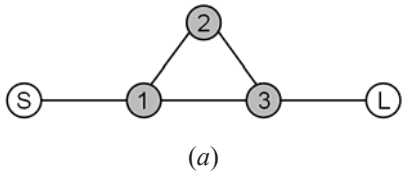

(*a*)

$$\begin{bmatrix} 0 & 1.077 & 0 & 0 & 0 \\ 1.077 & 0 & 0.962 & 0.413 & 0 \\ 0 & 0.962 & -0.495 & 0.962 & 0 \\ 0 & 0.413 & 0.962 & 0 & 1.077 \\ 0 & 0 & 0 & 1.077 & 0 \end{bmatrix}$$

(*b*)

Fig. 3. Three-pole filter with a zero in the upper stop-band: (*a*) topology of the filter; (*b*) coupling matrix of the filter.

design of complex circuits by adopting one simple filament material. Moreover, loss tangent of the material is lowered: this permits increasing the quality factor of cavity filters even by using the same material.

To demonstrate this concept, two substrate integrated waveguide (SIW) filters [8] with the same topology and frequency response have been designed and fabricated by 3D printing. One filter is based on a dielectric substrate printed with 100% infill (Fig. 1*a*), whereas in the second filter the input/output SIW lines are fabricated with 100% infill and the resonant cavities are made with 40% infill. This solution allows to increase the quality factor of the filter, at the cost of a slightly increase footprint size.

II. Local Control of the Dielectric Permittivity

FDM allows local modification of the printed material properties, mainly by acting on the infill factor [7]. The variation of the density affects the effective dielectric permittivity of the printed material as well as its electric loss tangent. The effect of the material density on the dielectric properties of the material can be accurately estimated by adopting the Bruggeman's model [7].

In this work, ABS filament with dielectric permittivity ε_r=2.7 and loss tangent $\tan\delta$=0.02 has been adopted. According to the Bruggeman's model, the results shown in Fig. 2 can be achieved when varying the infill factor. When using 40% infill factor, for instance, the dielectric permittivity is reduced to ε_r=1.6, and this determined an increase in the circuit dimensions. However, the loss tangent is simultaneously reduced to $\tan\delta$=0.008, with a consequent increase in the quality factor of the resonant cavities.

III. 3D Printed SIW Filters

Let us consider a three-pole filter having a fractional bandwidth (FBW) of 4%, centered at the frequency of 3.86 GHz and having a transmission zero in the upper stop-band. Such a filter has been synthetized by using the topology of Fig. 3*a*. The relevant coupling matrix is shown in Fig. 3*b*.

Two different filters implementing this coupling matrix have been designed. As shown in Fig. 1*a*, the first filter was designed by using a dielectric substrate with permittivity ε_r=2.7, corresponding to 100% infill. In this filter, the dielectric permittivity is homogeneous in the whole structure. On the contrary, in the second filter (Fig. 1*b*), the permittivity of the cavity resonators is decreased to ε_r=1.6, corresponding to 40% infill, while the permittivity is kept to ε_r=2.7 in the input/output waveguides. Both filters have been designed to obtain the same frequency response. This means that the cavities of the second filter (with lower permittivity) are larger than those of the first filter (with higher permittivity). Both filters have been realized in SIW technology, and the optimization has been performed by using the commercial FEM solver Ansys HFSS.

The geometrical structure is the same for both filters and it is illustrated in Fig. 1. It consists of three cylindrical cavity resonators fed by rectangular waveguides. The resonant mode in each cylindrical cavity is the $TM^z_{0,1,0}$ mode. Each resonator is connected to the other two resonators through inductive irises to realize the coupling scheme of Fig. 3*a*. The width of irises is chosen to realize the required coupling coefficient according to the coupling matrix in Fig. 3*b*.

The simulation results of the optimized filters are shown in Fig. 4. In particular, the scattering parameters of the first filter are reported in Fig. 4*a*: the insertion loss of the filter is approximately 7.3 dB at 3.86 GHz. Conversely, the second filter, whose frequency response is shown in Fig. 4*b*, exhibits an insertion of 3.7 dB, which is definitely smaller than the loss of the first filter. On the other hand, the diameter of the resonant cavities is 19.2 mm in the first filter and it is increase to 24.4 mm in the second filter.

IV. 3D Printing Manufacturing Process

The HFSS models are exported as STEP files, which are then re-imported into Solidworks and re-exported into .STL files, which are standard for 3D printing. The models are then sliced, turning 3D models into layer-by-layer gcode, which contain the path and flow rate the heated extruder must follow. A slicer that allows the ability to slice different parts of a

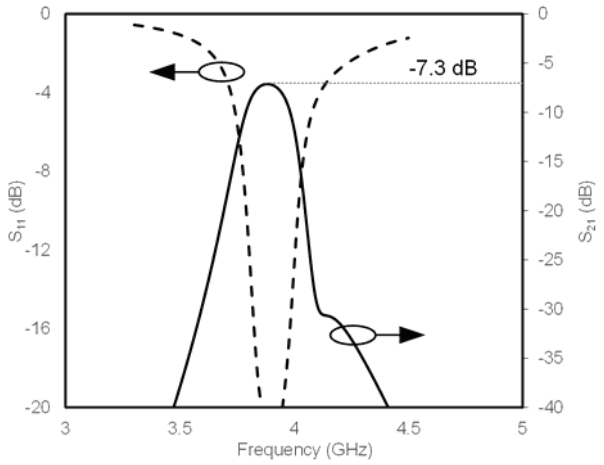

(*a*)

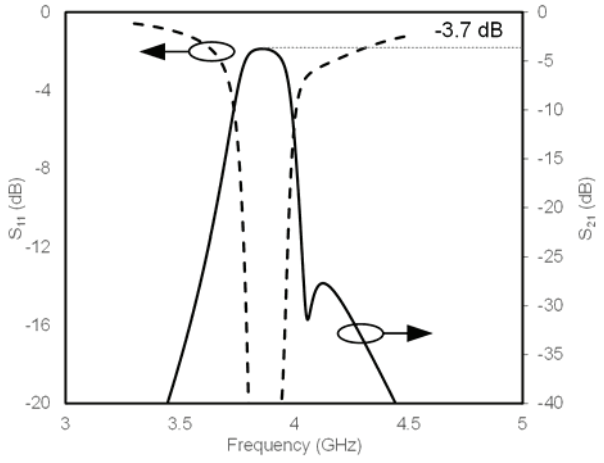

(*b*)

Fig. 4. Simulation results: (*a*) simulated scattering parameters of the first filter (100% infill); (*b*) simulated scattering parameters of the second filter (40% infill).

model with different profiles with a single nozzle was necessary, and thus Simplify3D was used for generation of the gcode.

Hatchbox branded acrylonitrile butadiene styrene (ABS) is printed on a Printrbot Metal Plus with 127 μm layers at 235 °C on a 95 °C heated build plate to reduce warping of the ABS material (Fig. 5). This layer height is used to improve print quality as it is an integer multiple related to the full step size of the stepper motor and pitch of the z-axis threaded rod. A nozzle with 0.4 mm diameter was used with trace widths of 0.42 mm. Special care is needed at the interface between regions with different infill (Fig. 6).

As a last step, the printed dielectric substrate is metalized using copper tape and rivets, which are then soldered together, to create the top/bottom conductive layers as well as the sidewalls of the SIW structure.

The fabricated prototypes of the two SIW filters described in Sec. III are shown in Fig. 7, after the application of the copper tape, the rivets, and the coaxial connectors.

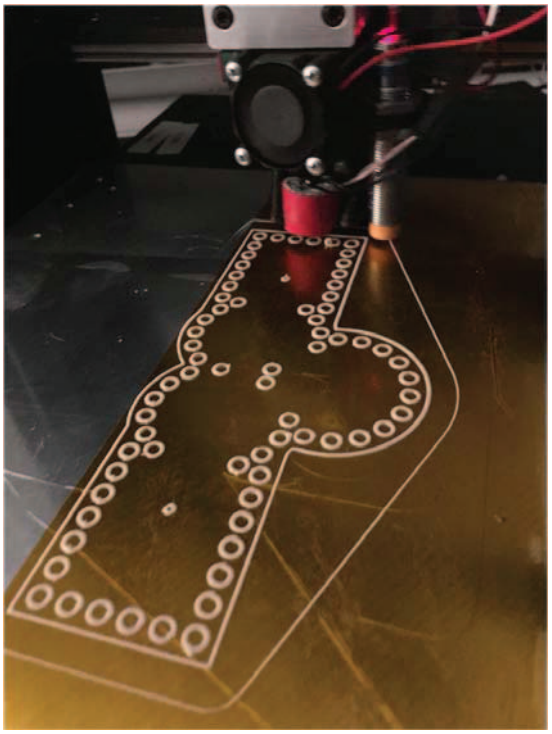

Fig. 5. Printing of first layer with DuPont Kapton tape on Printrbot Metal Plus.

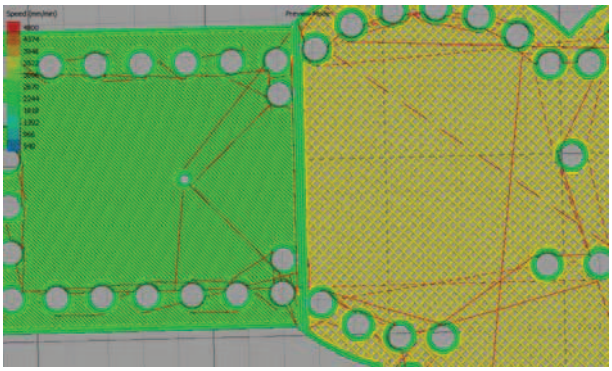

Fig. 6. Simplify3D gcode preview demonstrating the 40% infill portion vs the 100% infill portion.

V. Experimental Results

The experimental results of the two filters in terms of scattering parameters are shown in Fig. 8.

In the first filter with 100% infill (Fig. 8*a*), the simulated and measured results vary by 2.7 dB at the peak, but otherwise agrees well with simulated results shown in Fig. 4*a*. A minor frequency shift in the frequency response of the first filter may be attributed to several possible causes. While the model was printed on 0.4 mm nozzle for balance between print speed and quality, a 0.2 mm nozzle may benefit the print by reducing surface roughness and error of infill amount.

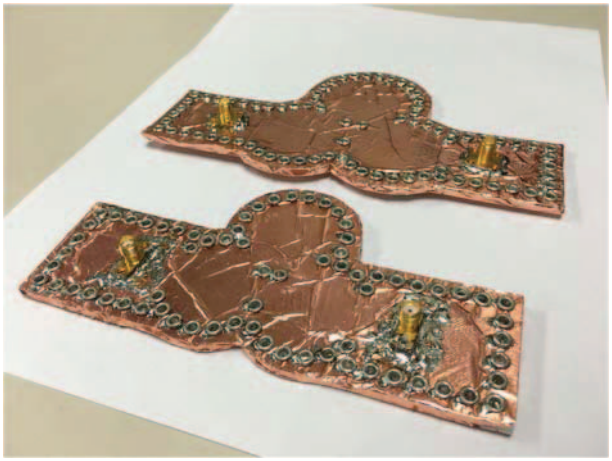

Fig. 7. Both SIW Filters with the single infill model (bottom), multi-infill model (top).

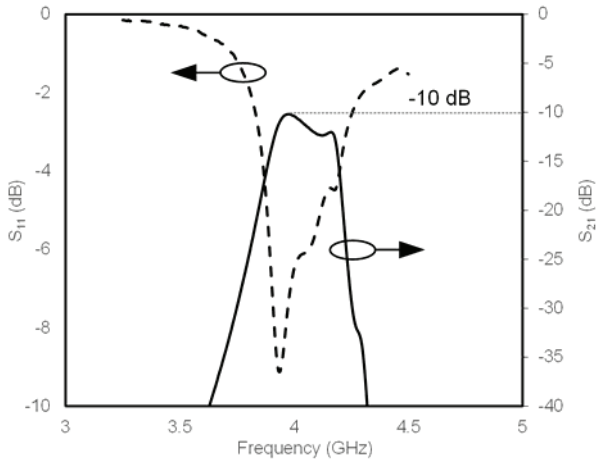

(*a*)

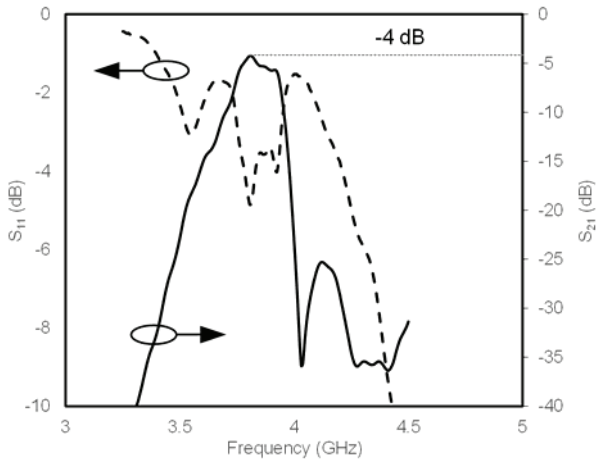

(*b*)

Fig. 8. Experimental results: (*a*) measured scattering parameters of the first filter (100% infill); (*b*) measured scattering parameters of the second filter (40% infill).

The second filter, based on two regions with different dielectric permittivity (Fig. 8*b*), had significant lower measured losses (approximately 4 dB insertion loss compared to 10 dB of the first filter). Moreover, measured losses vary only by 0.3 dB at the peak with respect to simulations (reported in Fig. 4*b*).

If there is a deviation in infill flow rates that results in 101% infill the nozzle may collide with the over flowing material causing material to burn, loss of print quality, or knocking the print off the build plate. Both the surface roughness and need to print below 101% may cause undesired minor variations in dielectric constant leading to a slight frequency shift.

VI. Conclusion

This paper demonstrates the feasibility of a new method for the fabrication of SIW filters by additive manufacturing. This technique allows fast prototyping, large flexibility (even to extended to shapes that are non-planar), and very low fabrication cost (in this case, the dielectric costs of a single print of one of these filters was 0.35 €).

Moreover, the possibility of using one single filament material to tune the dielectric permittivity as well as the electric loss tangent was theoretical and experimentally demonstrated. This solution paves the road to many components, even in cases where the current losses associated with the filament material may be considered too high.

A variety of materials exist for 3D printing, and in combination with multi-material printing a wide range of filter designs with near limitless physical layout could be achieved.

References

[1] C. Chua, K. Leong, and C. Lim, *Rapid Prototyping: Principles and Applications*, River Edge (NJ), USA, 2003.

[2] H. Lipson and M. Kurman, *Fabricated: The New World of 3D Printing*, John Wiley & Sons, 2013.

[3] E. MacDonald *et al*., "3D Printing for the Rapid Prototyping of Structural Electronics," *IEEE Access*, Vol. 2, pp. 234-242, Dec. 2014.

[4] J.G. Hester *et al*., "Additively Manufactured Nanotechnology and Origami-Enabled Flexible Microwave Electronics," *Proceedings of the IEEE*, Vol. 103, No. 4, pp. 583-606, April 2015.

[5] S. Moscato, R. Bahr, T. Le, M. Pasian, M. Bozzi, L. Perregrini, and M.M. Tentzeris, "Additive Manufacturing of 3D Substrate Integrated Waveguide Components," *Electronics Letters*, Vol. 51, No. 18, pp. 1426-1428, Sept. 2015.

[6] M. Bozzi, S Moscato, L. Silvestri, N. Delmonte, M. Pasian, and L. Perregrini, "Innovative SIW Components on Paper, Textile, and 3D-Printed Substrates for the Internet of Things," *2015 Asia-Pacific Microwave Conference* (APMC2015), Nanjing, China, Dec. 6–9, 2015

[7] S. Moscato, R. Bahr, T. Le, M. Pasian, M. Bozzi, L. Perregrini, and M.M. Tentzeris, "Infill Dependent 3D-Printed Material Based on NinjaFlex Filament for Antenna Applications," *IEEE Antennas and Wireless Propagation Letters*, Vol. 15, pp. 1506-1509, 2016.

[8] M. Bozzi, A. Georgiadis, and K. Wu, "Review of Substrate Integrated Waveguide (SIW) Circuits and Antennas," *IET Microwaves, Antennas and Propagation*, Vol. 5, No. 8, pp. 909–920, June 2011.